Journal of Macromolecular Science, Part A
Publication details, including instructions for authors and subscription information:
http://www.informaworld.com/smpp/title~content=t713597274

Mathematical Modeling of PVC Suspension Polymerization: A Unifying Approach and Some new Results

E. Sidiropoulou[a]; C. Kiparissides[a]
[a] Department of Chemical Engineering, Chemical Process Engineering Research Institute, Aristotle University of Thessaloniki, Thessaloniki, Greece

To cite this Article Sidiropoulou, E. and Kiparissides, C.(1990) 'Mathematical Modeling of PVC Suspension Polymerization: A Unifying Approach and Some new Results', Journal of Macromolecular Science, Part A, 27: 3, 257 — 288
To link to this Article: DOI: 10.1080/00222339009349551
URL: http://dx.doi.org/10.1080/00222339009349551

J. MACROMOL. SCI.—CHEM., A27(3), pp. 257–288 (1990)

MATHEMATICAL MODELING OF PVC SUSPENSION POLYMERIZATION: A UNIFYING APPROACH AND SOME NEW RESULTS

E. SIDIROPOULOU and C. KIPARISSIDES*

Department of Chemical Engineering and Chemical Process Engineering Research Institute
Aristotle University of Thessaloniki
Thessaloniki, 54006, Greece

ABSTRACT

The aim of the present investigation is the development of a unifying framework for modeling free-radical suspension and bulk vinyl chloride polymerizations. A fairly comprehensive but realistic model is described that has the ability to predict the rate of polymerization as well as the molecular properties of polymer as a function of the process conditions. It is shown that no significant differences exist between the predictions of the present model and those obtained by various well-known two-phase PVC models published before. In addition to the prediction of fractional monomer conversion and rate of polymerization, the new model predicts the anomalous structures observed in commercial PVC, namely, the number of short- and long-chain branches as well as the number of unsaturated terminal double bonds per polymer molecule. Simulation results show that the present model provides realistic predictions of the important molecular properties in agreement with experimental observations reported in the literature. Finally, the validity of the quasi-steady-state approximation for growing macroradicals is tested by comparing conversion and molecular weight results obtained with or without its application.

KINETICS OF VCM POLYMERIZATION

Vinyl chloride (VC) polymerization is a multiphase (heterogeneous) process. Its key feature is that poly(vinyl chloride) (PVC) is practically insoluble in its monomer, the equilibrium solubility of PVC being approximately 0.1 wt%.

For the derivation of the rate expressions and polymer quality equations, one can assume that the polymerization of VC takes place in three stages. During the first stage, which extends from zero to about 0.1% conversion, the reaction mixture consists mainly of pure monomer, the concentration of polymer being less than its solubility limit. Stage 2 extends from the point of the appearance of the polymer-rich phase (0.1%) to a fractional conversion x_c (0.7–0.8) at which the separate monomer phase disappears. During this stage, the reaction mixture will consist of two separate phases, the monomer-rich phase and the polymer-rich phase. The reaction takes place in both phases at different rates and is accompanied by transfer of monomer from the monomer phase to the polymer phase, so that the composition of the latter is kept constant. The disappearance of the separate monomer phase is associated with a pressure drop in the reactor. In the conversion range $x_c < x < 1.0$, we have once again a homogeneous system consisting of the polymer phase swollen with monomer. During this stage, the monomer mass fraction in the polymer phase will decrease as the total monomer conversion approaches a final limiting value.

In the present study the monomer-rich phase will be denoted as Phase 1 and the polymer-rich phase as Phase 2. In any two-phase system the overall molar species rate will be equal to the sum of the species rates in the two phases. These can be calculated by applying simple homogeneous kinetics to each phase and assuming that the kinetic mechanism of free-radical polymerization of vinyl chloride can be described in terms of the following elementary reactions:

Initiation:

$$\mathrm{I} \xrightarrow{k_{dj}} 2\mathrm{I}^*$$

$$\mathrm{I}^* + \mathrm{M} \xrightarrow{k_{ij}} \mathrm{R}_1$$

Propagation:

$$\mathrm{R}_x + \mathrm{M} \xrightarrow{k_{pj}} \mathrm{R}_{x+1}$$

Transfer to monomer:

$$\mathrm{R}_x + \mathrm{M} \xrightarrow{k_{tmj}} \mathrm{P}_x + \mathrm{R}_1$$

Transfer to polymer:

$$R_x + P_y \xrightarrow{k_{tpj}} P_x + R_y$$

Intramolecular transfer:

$$R_x \xrightarrow{k_{bj}} R_x$$

Termination reactions:

$$R_x + R_y \xrightarrow{k_{tdj}} P_x + P_y$$

$$R_x + R_y \xrightarrow{k_{tcj}} P_{x+y}$$

I, M, R_x, and P_x denote the initiator, monomer, live, and dead polymer molecules of chain length x, respectively, and k_{dj}, k_{pj}, k_{tmj}, etc. are the corresponding rate constants in the above elementary reactions associated with Phase j.

The initiation process, similarly to other free-radical vinyl polymerizations, involves the chemical decomposition of unstable peroxides or azo compounds into free radicals which can react rapidly with monomer to begin the propagation of a polymer chain. The overall initiator concentration will be related to the initiator concentrations in the two phases according to

$$[I] = [I_1]\phi_1 + [I_2]\phi_2, \tag{1}$$

where ϕ_j is the volume fraction of Phase j in the two-phase system and $[I_j]$ denotes the corresponding initiator concentration. The initiator distribution between the two phases is usually expressed in terms of an initiator partition coefficient,

$$K_I = [I_2]/[I_1]. \tag{2}$$

In general, the initiator decomposition rate constants can be considered to be equal in the two phases. Similarly, the monomer distribution in the two phases will be given by

$$K_M = [M_2]/[M_1], \quad (3)$$

where K_M represents the monomer partition coefficient.

Transfer to monomer and polymer reactions are very important in VC polymerization since their frequency relative to the chain propagation reaction controls the molecular weight. Transfer to monomer causes a shift of the molecular weight distribution (MWD) to lower values. On the other hand, transfer to polymer can lead to the formation of branched polymers, which causes a shift of the MWD to higher values. Hjertberg and Sörvik [1] and Hamielec et al. [2] found that, at high conversions, under monomer starvation conditions, the amount of low molecular weight species as well as long-chain branching (LCB) and short-chain branching (SCB) increased.

The nature and mechanism of formation of so-called anomalous structures (chain defects) in PVC has been the subject of numerous studies over the past 10 years (Caraculacu [3], Starnes et al. [4], Hjertberg and Sörvik [5, 6]). Transfer to monomer and intramolecular (backbiting) reactions are considered to be responsible for the formation of the short side chains observed in PVC. Note that transfer reactions do not change the total number of live polymer chains and, therefore, the rate of polymerization and the number-average molecular weight will not be affected.

The double bond content in PVC resins has been found to vary in the range of 1.5 to 4.0 per 1000 VC units. Hildenbrand et al. [7] found that the number of double bonds per unit weight of polymer increases as the polymerization temperature increases and is proportional to the number of polymer molecules. Double bond defects can arise from both transfer to monomer and termination by disproportionation. These bonds are called "terminal double bonds" and are located at, or close to the ends of, polymer chains. The various anomalous and unsaturated structures found in PVC resins are considered to be the primary cause for the low thermal stability of the polymer.

Termination by disproportionation is believed to be the principal termination mechanism in VC polymerization. This is supported by the fact that molecular weight measurements show a polydispersity ratio ($\bar{M}_w/\bar{M}_n$) very close to 2.0, indicative of the predominance of the disproportionation mechanism. Termination reactions involving large molecules can become diffusion controlled even at low monomer conversions. The appearance of the gel effect results in a decrease of the termination rate constant which, in turn, can have a profound effect on the relative rates of free-radical reactions and the molecular structure of polymer chains. At high monomer conversions, even the propagation rate constant can become diffusion controlled. This leads to the formation of low molecular weight chains and increases the frequency of long-chain branching. Furthermore, if the polymerization temperature is below the glass-transition temperature of the monomer/polymer mixture, a limiting conversion

(<100%) may prevail due to the transition of the reaction mixture into the glassy state. The effect of diffusion-controlled phenomena on VC polymerization at high conversions has been investigated by Hamielec et al. [2].

In what follows, a brief review of previous mathematical models proposed for the suspension and bulk polymerization of vinyl chloride is presented.

REVIEW OF PREVIOUS MODELS

Over the past 20 years, several mathematical models have been developed to describe the two-phase polymerization of VC in suspension and bulk reactors. The key feature in all these models is that PVC is practically insoluble in its monomer, and polymerization proceeds simultaneously in the two phases almost from the start of the reaction. These models have been described in two review papers by Ugelstad and coworkers [8, 9].

The first two-phase model that appeared in the open literature was that of Talamini et al. [10]. Talamini's model assumes that no transfer of radicals takes place between the two phases, and the initiator concentration remains constant. Later Abdel-Alim and Hamielec [11] modified this model by taking into account the change in the volumes of the two phases as well as the change in the initiator concentration with reaction time. Moreover, Abdel-Alim and Hamielec's model accounted for the diffusion control of the propagation and termination reactions at high conversions.

Contrary to the last two models, Ugelstad et al. [12] proposed a kinetic model that accounts for transfer of radicals between the two phases. The main difference between Ugelstad's model and Kuchanov and Bort's model [13] is that the latter does not make use of the assumption of equilibrium distribution of radicals between the two phases.

A kinetic model that takes into account the formation of precipitated radicals was proposed by Olaj [14]. However, Olaj's model does not account for the termination of dissolved radicals in the monomer phase. More recently, Thiele et al. [15] and Kafarov et al. [16] proposed new modified two-phase models that take into account the mass transfer of radicals between the two phases.

By far the most comprehensive model published on PVC is that of Kelsall and Maitland [17]. Their model takes into account the mass transfer of various species (i.e., initiator, monomer, polymer) between the different phases and the possibility of inhomogeneous initiator distribution and efficiency. A detailed description of the polymer precipitation and growth processes is also included. The model contains a considerable number of unknown parameters, which might complicate its application to commercial PVC reactors.

The aim of the present paper is to develop a fairly comprehensive but realistic model for describing the suspension (bulk) polymerization of VC. In addition to the prediction of polymerization rate and molecular weight averages, the model should have the ability to predict the anomalous structures observed in PVC as a function of polymerization conditions.

GENERAL MATHEMATICAL MODEL DEVELOPMENT

The prediction of molecular weight distribution (MWD) and degree of branching distribution (DBD) in polymerizations has been the subject of numerous investigations over the past 40 years. One of the most successful methods for modeling free-radical polymerizations is the so-called method of moments (Tirell et al. [18]). The moment equations describe the molecular weight developments in a polymerization reactor and are usually derived from the original species balance equations through well-established mathematical techniques and the definition of the moments of the differential number chain-length distributions. The numerical solution of the resulting moment equations is straightforward and readily leads to the instantaneous and cumulative molecular weight averages. The method of moments can equally well be applied to both linear and branched polymers. In the present study, moment equations for both monomer and polymer phases are established. A mass-transfer term is included with each moment equation to account for the transfer of macroradicals between the two phases. In what follows, the rate functions for the net production of live and dead macromolecules of chain length x in each phase are first derived. Subsequently, moment differential equations are written for each phase to describe the molecular weight developments during the three stages of polymerization.

Polymerization Rate Functions

Let r_{xj}^* and r_x denote the net rates of production of live polymer chains of length x in Phase j and dead polymer chains of length x, respectively. The expressions for these rate functions can be obtained by combining the reaction rates of the various elementary reactions describing the generation and consumption of growing or dead polymer macromolecules of length x. Based on the above kinetic mechanism of free-radical polymerization of VC, the following general composite rate functions for r_{xj}^* and r_x can be derived:

$$\begin{aligned} r_{xj}^* = {} & (2f_j k_{dj}[\mathrm{I}_j] + k_{tmj}[\mathrm{M}_j]\Sigma_x[\mathrm{R}_{xj}])f(x) - k_{pj}[\mathrm{M}_j][\mathrm{R}_{xj}] - k_{tmj}[\mathrm{M}_j][\mathrm{R}_{xj}] \\ & - k_{tj}[\mathrm{R}_{xj}]\Sigma_x[\mathrm{R}_{xj}] + k_{pj}\mathrm{M}_j[\mathrm{R}_{x-1,j}]\,[1 - f(x)] - k_{tpj}([\mathrm{R}_{xj}]\Sigma_x x[\mathrm{P}_x] \\ & - x[\mathrm{P}_x](\Sigma_x[\mathrm{R}_{xj}])(1 - j), \end{aligned} \tag{4}$$

$$r_x = \Sigma_j(k_{tmj}[M_j][R_{xj}]) + \Sigma_j[k_{tj}[R_{xj}](\Sigma_x[R_{xj}])] + k_{tp2}([R_{x2}]\Sigma_x x[P_x] - x[P_x]\Sigma_x[R_{x2}]), \quad (5)$$

where $[R_{xj}]$ represents the concentration of live polymer chains of length x in Phase j. $f(x)$ is a Dirac delta function expressed as

$$f(x) = \begin{cases} 1 & \text{if } x = 1 \\ 0 & \text{if } x > 1. \end{cases} \quad (6)$$

Equation (5) represents the overall rate of dead polymer production and is equal to the sum of the polymer production rates in the two phases.

As previously discussed, for modeling purposes it is often impractical to use the full differential NCLDs of live and dead macromolecules to represent the state of the reacting system. Instead, it is more convenient to work with the leading moments of live and dead polymer distributions, which are defined as

$$[\lambda_{ij}] = \Sigma_x x^i[R_{xj}] \quad j = 1, 2 \quad \text{and} \quad i = 0, 1, 2, \ldots, \quad (7)$$

$$[\mu_i] = \Sigma_x x^i[P_x]. \quad (8)$$

The introduction of the moments of the NCLDs results in the reduction of the original infinite set of species balance equations into a simple set of six or nine coupled moment differential equations. The corresponding reaction rates $(r_\lambda)_{ij}$ and $(r_\mu)_i$ for the leading moments of the live and dead polymer distributions can be obtained from Eqs. (4) and (5) by multiplying each term by x^i and summing the resulting expressions over the total variation of x.

$$(r_\lambda)_{ij} = \Sigma_x x^i r_{xj}{}^* = 2f_j k_{dj}[I_j] + k_{tmj}[M_j]([\lambda_{0j}] - [\lambda_{ij}]) + k_{pj}[M_j]i[\lambda_{i-1,j}] - k_{tj}[\lambda_{0j}][\lambda_{ij}] - k_{tpj}([\mu_1][\lambda_{ij}] - [\mu_{i+1}][\lambda_{0j}])(1 - j). \quad (9)$$

$$(r_\mu)_i = \Sigma x^i r_x = \Sigma_j(k_{tmj}[M_j][\lambda_{ij}]) + \Sigma_j(k_{tj}[\lambda_{0j}]\lambda_{ij}] + k_{tp2}([\mu_1][\lambda_{i2}] - [\mu_{i+1}][\lambda_{02}]). \quad (10)$$

As it will become apparent in the following section, one can easily calculate the instantaneous and cumulative number- and weight-average molecular weights in terms of the leading moments of the live and dead NCLDs.

In any two-phase system the overall monomer consumption rate will be given by the sum of the polymerization rates in each phase:

$$r_p = r_{p1}\phi_1 + r_{p2}\phi_2. \tag{11}$$

Assuming that the long-chain approximation (LCA) is valid, that is, monomer consumed in reactions other than propagation is negligible, one can obtain the following expression for the monomer consumption rate in Phase j, r_{pj}:

$$r_{pj} = k_{pj}[M_j][\lambda_{0j}]. \tag{12}$$

Similarly, the total initiator consumption rate will be given by

$$r_d = r_{d1}\phi_1 + r_{d2}\phi_2 \tag{13}$$

where r_{dj} is the initiator consumption rate in Phase j:

$$r_{dj} = k_{dj}[I_j]. \tag{14}$$

A Detailed Batch Reactor Model

Based on the kinetic mechanism of VC polymerization and the derived polymerization rate functions, one can proceed with the development of a general mathematical framework to describe the heterophase polymerization (suspension, bulk) of VC in a batch reactor. The present model assumes a two-phase polymerization occurring in three distinct stages. Accordingly, mass balance equations for initiator, monomer, and the leading moments of MWD are derived for each stage of polymerization.

Stage I: $0 < x < 0.1\%$

During this stage the polymerization takes place only in the monomer phase. The mass balance equations for initiator, monomer, and leading moments of NCLD are written as:

Mass balance for initiator:

$$dI_1/dt = -k_{d1}I_1;\ I_1(0) = I_0. \tag{15}$$

Mass balance for monomer:

$$dM_1/dt = -k_{p1}M_1[\lambda_{01}];\ M_1(0) = M_0. \tag{16}$$

Moment balances for live polymer radicals:

$$d\lambda_{01}/dt = 2f_1k_{d1}I_1 - k_{t1}\lambda_{01}^2/V_1, \tag{17}$$

$$d\lambda_{11}/dt = 2f_1k_{d1}I_1 - k_{t1}\lambda_{01}\lambda_{11}/V_1 + k_{tm1}[M_1](\lambda_{01} - \lambda_{11}) + k_{p1}[M_1]\lambda_{01}, \tag{18}$$

$$d\lambda_{21}/dt = 2f_1k_{d1}I_1 - k_{t1}\lambda_{01}\lambda_{21}/V_1 + k_{tm1}[M_1](\lambda_{01} - \lambda_{21}) + 2k_{p1}[M_1]\lambda_{11}. \tag{19}$$

On the assumption that the QSSA can be applied to the growing polymer chains, Eqs. (17)–(19) become

$$[\lambda_{01}] = (2f_1k_{d1}I_1/k_{t1})^{1/2}, \tag{20}$$

$$[\lambda_{11}] = [2f_1k_{d1}I_1 + (k_{tm1} + k_{p1})M_1[\lambda_{01}])/(k_{t1}\lambda_{01} + k_{tm1}M_1), \tag{21}$$

$$[\lambda_{21}] = (2f_1k_{d1}I_1 + k_{tm1}M_1[\lambda_{01}] + 2k_{p1}M_1[\lambda_{11}])/(k_{t1}\lambda_{01} + k_{tm1}M_1). \tag{22}$$

Moment balances for dead polymer chains are

$$d\mu_0/dt = k_{tm1}M_1[\lambda_{01}] + k_{t1}[\lambda_{01}]^2V_1, \tag{23}$$

$$d\mu_1/dt = k_{tm1}M_1[\lambda_{11}] + k_{t1}[\lambda_{01}][\lambda_{11}]V_1, \tag{24}$$

$$d\mu_2/dt = k_{tm1}M_1[\lambda_{21}] + k_{t1}[\lambda_{01}][\lambda_{21}]V_1. \tag{25}$$

Transfer to polymer is assumed to be insignificant during this stage. V_1 represents the volume of monomer Phase 1 and is practically constant during Stage I. Finally, the fractional monomer conversion can be calculated by

$$dx/dt = k_{p1}(1 - x)[\lambda_{01}]. \tag{26}$$

Note that in the above equations the symbols s_j and $[s_j]$ denote the amount of s in moles and the concentration of Species s in Phase j in mol/L, respectively.

Stage II: 0.1% $< x \leq x_c$

During this stage the polymerization occurs in two separate phases. Therefore, species mass balances are derived for each phase. The total initiator and monomer balances will be given by the sum of the corresponding species balances derived for

each phase. The two separate phases exist until a fractional conversion x_c has been reached at which the monomer-rich phase disappears. The concentration of monomer in each phase will remain constant and will be given by Eqs. (27) and (28):

$$[M_1] = \rho_m/(MW), \tag{27}$$

$$[M_2] = A\rho_m/[(MW)(A + \rho_m/\rho_p)], \tag{28}$$

where

$$A = (1 - x_c)/x_c. \tag{29}$$

Total initiator mass balance:

$$dI/dt = -k_{d1}I_1 - k_{d2}I_2. \tag{30}$$

Total monomer mass balance:

$$dM/dt = -k_{p1}[M_1]\lambda_{01} - k_{p2}[M_2]\lambda_{02}. \tag{31}$$

Moment balances for live polymer radicals:

$$d\lambda_{0j}/dt = 2f_jk_{dj}I_j - k_{tj}\lambda_{0j}^2/V_j + (-1)^jF([\lambda_{01}],[\lambda_{02}]), \tag{32}$$

$$d\lambda_{1j}/dt = 2f_jk_{dj}I_j - k_{tj}\lambda_{0j}\lambda_{1j}/V_j + k_{tmj}[M_j](\lambda_{0j} - \lambda_{1j}) + k_{pj}[M_j]\lambda_{0j} - k_{tpj}(\mu_1\lambda_{1j}/V_j - \mu_2\lambda_{0j}/V_j)(1 - j) + (-1)^jF([\lambda_{11}],[\lambda_{12}]), \tag{33}$$

$$d\lambda_{2j}/dt = 2f_jk_{dj}I_j - k_{tj}\lambda_{0j}\lambda_{2j}/V_j + k_{tmj}[M_j](\lambda_{0j} - \lambda_{2j}) + 2k_{pj}[M_j]\lambda_{1j} - k_{tpj}(\mu_1\lambda_{2j}/V_j - \mu_3\lambda_{0j}/V_j)(1 - j) + (-1)^jF([\lambda_{21}],[\lambda_{22}]). \tag{34}$$

The term $F([\lambda_{i1}],[\lambda_{i2}])$ represents the mass transfer of growing radicals between the two phases. Notice that Eqs. (32)–(34) can be considerably simplified by assuming that the QSSA holds good.

Total moment balances for dead polymer chains:

$$d\mu_0/dt = \Sigma_j(k_{tmj}[M_j]\lambda_{0j}) + \Sigma_j(k_{tj}\lambda_{0j}^2/V_j), \tag{35}$$

$$d\mu_1/dt = \Sigma_j(k_{tmj}[M_j]\lambda_{1j}) + \Sigma_j(k_{tj}\lambda_{0j}\lambda_{1j}/V_j) + k_{tp2}(\mu_1\lambda_{12}/V_2 - \mu_2\lambda_{02}/V_2), \quad (36)$$

$$d\mu_2/dt = \Sigma_j(k_{tmj}[M_j]\lambda_{2j}) + \Sigma_j(k_{tj}\lambda_{0j}\lambda_{2j}/V_j) + k_{tp2}(\mu_1\lambda_{22}/V_2 - \mu_3\lambda_{02}/V_2). \quad (37)$$

The fractional monomer conversion can be calculated as

$$dx/dt = k_{p1}[\lambda_{01}](1 - x - Ax) + k_{p2}[\lambda_{02}]Ax \quad (38)$$

V_1 and V_2 denote the volume of the monomer- and polymer-rich phase, respectively:

$$V_1 = V_0(1 - x - Ax), \quad (39)$$

$$V_2 = V_0x(A + \rho_m/\rho_p). \quad (40)$$

Stage III: $x_c < x$

For conversions greater than x_c, the polymerization takes place only in the polymer-rich phase. During this stage the following mass balance equations can be derived:

Mass balance for initiator:

$$dI_2/dt = -k_{d2}I_2. \quad (41)$$

Total monomer mass balance:

$$dM_2/dt = -k_{p2}M_2[\lambda_{02}]. \quad (42)$$

Moment balances for live polymer radicals:

$$d\lambda_{02}/dt = 2f_2k_{d2}I_2 - k_{t2}\lambda_{02}^2/V_2, \quad (43)$$

$$d\lambda_{12}/dt = 2f_2k_{d2}I_2 - k_{t2}\lambda_{02}\lambda_{12}/V_2 + k_{tm2}[M_2](\lambda_{02} - \lambda_{12}) + k_{p2}[M_2]\lambda_{02} - k_{tp2}(\mu_1\lambda_{12}/V_2 - \mu_2\lambda_{02}/V_2), \quad (44)$$

$$d\lambda_{22}/dt = 2f_2k_{d2}I_2 - k_{t2}\lambda_{02}\lambda_{22}/V_2 + k_{tm2}[M_2](\lambda_{02} - \lambda_{22}) + 2k_{p2}[M_2]\lambda_{12} - k_{tp2}(\mu_1\lambda_{22}/V_2 - \mu_3\lambda_{02}/V_2). \quad (45)$$

Assuming again that the QSSA is valid, Eqs. (43)–(45) can be replaced by the corresponding algebraic equations.

Total moment balances for dead polymer chains:

$$d\mu_0/dt = k_{tm2}[M_2]\lambda_{02} + k_{t2}\lambda_{02}^2/V_2, \quad (46)$$

$$d\mu_1/dt = k_{tm2}[M_2]\lambda_{12} + k_{t2}\lambda_{02}\lambda_{12}/V_2 + k_{tp2}(\mu_1\lambda_{12} - \mu_2\lambda_{02})/V_2, \quad (47)$$

$$d\mu_2/dt = k_{tm2}[M_2]\lambda_{22} + k_{t2}\lambda_{02}\lambda_{22}/V_2 + k_{tp2}(\mu_1\lambda_{22} - \mu_3\lambda_{02})/V_2, \quad (48)$$

The fractional monomer conversion can be calculated as

$$dx/dt = k_{p2}(1 - x)[\lambda_{02}]. \quad (49)$$

V_2 is given by

$$V_2 = V_0(1 - x + x\rho_m/\rho_p). \quad (50)$$

Polymer Quality Equations

In terms of the leading moments of the dead polymer chain-length distribution, one can calculate the instantaneous and cumulative number- and weight-average chain lengths. It can be shown that the instantaneous number-average chain length, x_{nj}, in Phase j will be given by

$$x_{nj} = (d\mu_{1j}/dt)/(d\mu_{0j}/dt). \quad (51)$$

Similarly, the instantaneous weight-average chain length, x_{wj}, can be calculated by

$$x_{wj} = (d\mu_{2j}/dt)/(d\mu_{1j}/dt). \quad (52)$$

The instantaneous averages will generally be different in the two phases. Therefore, one must use the following expressions to calculate the overall instantaneous

average chain lengths in terms of the rates of polymerization in the two phases:

$$\bar{x}_{n,i} = r_p/\Sigma_j(r_{pj}/x_{nj}), \tag{53}$$

$$\bar{x}_{w,i} = \Sigma_j(r_{pj}x_{wj})/r_p\,. \tag{54}$$

The cumulative number- and weight-average chain lengths can be directly expressed in terms of the moments of the polymer NCLD:

$$\bar{X}_n = \Sigma_x(xP_x)/\Sigma_x P_x = \mu_1/\mu_0, \tag{55}$$

$$\bar{X}_w = \Sigma_x(x^2P_x)/\Sigma_x(xP_x) = \mu_2/\mu_1. \tag{56}$$

The corresponding instantaneous and cumulative molecular weight averages are obtained by multiplying the chain length averages by the molecular weight of the monomer.

The nature and relative quantities of short- and long-chain branches along the PVC polymer chains have been extensively investigated. In general, PVC samples are found to contain 4–5 chloromethyl branches per 1000 monomer units. The concentration of ethyl and *n*-butyl branches is considerably lower. Long-chain branches (LCB) in PVC may arise by transfer to polymer. Törnell [19] suggested that chain transfer to polymer by both chlorine atoms and growing macroradicals can explain the formation of LCB in PVC. In spite of the progress made in explaining the formation of short- and long-chain branches in PVC, the now accepted mechanisms of transfer to monomer and polymer are very difficult to incorporate in a quantitative mathematical analysis of the polymerization due to the large number of unknown kinetic rate constants involved. In the present analysis it is assumed that transfer to polymer and intramolecular transfer reactions are responsible for the formation of SCB and LCB in PVC. This considerably simplifies the quantitative analysis of the polymerization since only two lumped rate constants, k_{tp} and k_b, need to be identified. Accordingly, the average number of long branches per polymer chain, $\bar{L}_n$, and the average number of short branches per chain, $\bar{S}_n$, can be obtained from the solutions of Eqs. (57) and (58), respectively:

$$d(\mu_0\bar{L}_n)/dt = M_0(k_{tp}/k_p)[x/(1-x)]dx/dt, \tag{57}$$

$$d\bar{S}_n/dt = k_b\lambda_0. \tag{58}$$

The corresponding LCB and SCB per 1000 monomer units will be given by

$$\text{LCB} = 1000(\bar{L}_n\mu_0/\mu_1), \tag{59}$$

$$SCB = 1000(\bar{S}_n \mu_0/\mu_1). \tag{60}$$

A UNIFYING ANALYSIS OF THE PREVIOUS PVC MODELS

In this section we present a unifying analysis of the main PVC reactor models published in the open literature. Our objective is to show that most well-known models developed before can be derived directly from the general model described in the previous section. Accordingly, the models of Abdel-Alim and Hamielec [11], Ugelstad et al. [12], Kuchanov and Bort [13], and Kelsall and Maitland [17] are compared to the present model, and their characteristic features are pointed out. For the sake of brevity we shall refer to these as Model A, B, C, and D in accordance with the order of the last citation.

Model A

Talamini et al. [10] were the first to derive a two-phase model to predict the time variation of fractional monomer conversion in a suspension (bulk) PVC reactor. The assumptions made in Talamini's model are:

i. The corresponding initiator decomposition and propagation rate constants as well as the initiator efficiencies in the two phases are equal.
ii. The QSSA for growing radicals holds true for both phases.
iii. The initiator concentration is the same in both phases.
iv. No transfer of radicals between the two phases occurs, $F(\lambda_{i1},\lambda_{i2}) = 0$.
v. The initiator concentration does not change with conversion.
vi. The volume of the reacting mixture remains constant.

Abdel-Alim and Hamielec [11] modified Talamini's model by replacing Assumptions (v) and (vi) with Assumptions (vii) and (viii), respectively:

vii. For an isothermal polymerization in a batch reactor, the initiator concentration changes with reaction time according to

$$[I] = [I_0] \exp(-k_d t)/(1 - Bx). \tag{61}$$

viii. The volume of the reacting mixture changes linearly with conversion:

$$V = V_0(1 - Bx);\ B = (\rho_p - \rho_m)/\rho_p \tag{62}$$

From Eq. (32) and Assumptions (i)–(iv) and (vii)–(viii), one obtains the following steady-state equations for the growing macroradicals:

$$[\lambda_{0j}] = (2fk_d[I_0]/(k_{tj}(1 - Bx)))^{1/2} \exp(-k_d t/2), \quad j = 1, 2. \tag{63}$$

Substitution of Eqs. (63) into Eq. (38) yields Abdel-Alim and Hamielec's original expression for monomer conversion:

$$dx/dt = k_p(2fk_d[I_0]/(k_{t1}(1 - Bx)))^{1/2} \exp(-k_d t/2) (1 - x - Ax + PAx), \tag{64}$$

where P denotes the ratio of radical concentrations in the two phases:

$$P = [\lambda_{02}]/[\lambda_{01}] = (k_{t1}/k_{t2})^{1/2} \tag{65}$$

Equation (64) will be valid in the conversion range $0 < x \leq x_c$. In the conversion range $x_c < x < 1$, the appropriate expression for monomer conversion is directly obtained from homogeneous kinetics. To account for the fact that at high conversions the termination and propagation reactions become diffusion controlled, Abdel-Alim and Hamielec suggested the use of an empirical correction factor $(1 - x)/(1 - x_c)$. Thus, the following rate expression for the monomer conversion is obtained:

$$dx/dt = k_p(2fk_d[I_0]/(k_{t1}(1 - Bx)))^{1/2} \exp(-k_d t/2)P(1 - x)^2/(1 - x_c). \tag{66}$$

Abdel-Alim and Hamielec [11] used the instantaneous property method (Biesenberger and Sebastian [20]) to derive expressions for the molecular weight distribution and averages. Application of the QSSA and homogeneous kinetics to each phase yields the following equations for the instantaneous number- and weight-average chain lengths:

$$x_{nj} = 1/\tau_j; \; x_{wj} = 2/\tau_j, \tag{67}$$

where τ_j is defined as

$$\tau_j = d\mu_{0j}/d\mu_{1j} = k_{tm}/k_p + [2fk_dk_{t1}[I_0]/(1 - Bx)]^{1/2} \exp(-k_d t/2)/(P^{j-1}k_p[M_j]). \tag{68}$$

The overall instantaneous averages are given by Eqs. (53) and (54). Finally, the overall cumulative averages can be calculated by

$$\bar{X}_n = x/\int \Sigma_j (r_{pj}/r_p x_{nj})dx, \tag{69}$$

$$\bar{X}_w = (1/x)\int \Sigma_j (r_{pj} x_{wj}/r_p)dx. \tag{70}$$

Abdel-Alim and Hamielec's model has been successfully applied to several commercial PVC processes.

Model B

Ugelstad et al. [12] assumed production of radicals in both phases but in contrast to Model A they included the transfer of radicals between the two phases. However, they suggested that an equilibrium distribution of radicals is quickly established between the two phases and expressed the radical mass-transfer term in Eq. (32) as

$$F([\lambda_{01}],[\lambda_{02}]) = k_{ma}[\lambda_{01}] - k_{md}[\lambda_{02}] = 0, \tag{71}$$

where k_{ma} and k_{md} are the radical absorption and desorption mass-transfer coefficients, respectively. Application of QSSA to Eq. (32) yields the following expressions for the zero moments of the growing macroradical distributions:

$$[\lambda_{01}] = [2fk_d I/(k_{t1}V_1 + P^2 k_{t2}V_2)]^{1/2}, \tag{72}$$

$$[\lambda_{02}] = P[\lambda_{01}];\ P = k_{ma}/k_{md}. \tag{73}$$

Note that in Ugelstad's model, all but (iv) to (vi) of Talamini's assumptions hold good. Substitution of Eqs. (72) and (73) into Eq. (38), and assuming that V_1 and V_2 can be expressed by Eqs. (39) and (40), one can obtain Ugelstad's original expression for the fractional monomer conversion:

$$dx/dt = k_p[2fk_d[I]/(k_{t1}(1 - x - Ax) + P^2 k_{t2}x(A + \rho_m/\rho_p)))^{1/2} (1 - x - Ax + PAx). \tag{74}$$

Model C

Kuchanov and Bort [13] assumed that the radical desorption from Phase 2 can be completely neglected. Application of QSSA to Eq. (32) gives the following expressions for $[\lambda_{01}]$, $[\lambda_{02}]$:

$$[\lambda_{01}] = k_{ma}/(2k_{t1}V_1)[(1 + 8fk_d I_1 k_{t1}V_1/k_{ma}^2)^{1/2} - 1], \tag{75}$$

$$[\lambda_{02}] = [(k_{ma}[\lambda_{01}])^2 + 2fk_d I_2 k_{t2} V_2]^{1/2}/k_{t2}V_2. \quad (76)$$

Substitution of Eqs. (75) and (76) into Eq. (38) yields the Kuchanov-Bort expression for the time variation of the fractional monomer conversion:

$$dx/dt = k_p([\lambda_{01}](1 - x - Ax) + [\lambda_{02}]Ax). \quad (77)$$

Model D

In 1983 Kelsall and Maitland [17] proposed the most comprehensive model for the suspension polymerization of VC. A detailed description of this model can be found in the original paper of Kelsall and Maitland [17]. The model does not include any expressions related to the formation of anomalous structures observed in PVC. Furthermore, the model does not account for the diffusion control of propagation and termination rate constants at high monomer conversions.

As will become apparent in the following section, simulation results obtained by the various models do not show significant differences, which underlines the importance of the simpler models for engineering calculations related to the rate of polymerization and fractional monomer conversion.

DISCUSSION AND SIMULATION RESULTS

Simulation studies were carried out with the present model as well as with Models A–D to obtain a direct comparison for conversion and rate of polymerization results. Physical and kinetic rate constants used in all simulation studies are recorded in Table 1. Several simulation runs were also done with the present model to determine the effects of the various kinetic parameters and elementary reactions on the molecular structure of the polymer chains.

Conversion and Rate of Polymerization Results

To account for the dependence of termination and propagation rate constants on the temperature and polymer concentration, the diffusion-controlled models of Hamielec et al. [2] and Abdel-Alim and Hamielec [11] were utilized. Accordingly, the termination and propagation rate constants were expressed as

$$k_{t2} = k_{t20}((1 - x_f)/(1 - x))^2(k_p/k_{p0})^2, \quad (78)$$

$$k_p = k_{p0} \exp(-A(1/V_f - 1/V_{f,cr})). \quad (79)$$

TABLE 1. Physical Parameters and Kinetic Rate Constants for VC Polymerization

Physical Parameters:	
A =	0.2 L^{-1}
α =	−0.41591
β =	0.42642
I_0 =	0.2 mol
M_0 =	25.25 mol
T =	323 K
P =	27.0 − 0.14 (T − 273.16)
x_c =	0.85 − 0.0019 (T − 273.16)
Kinetic Rate Constants	
k_b =	$0.0115k_{tm}$ (at 50°C)
k_d =	6.32×10^{16} exp (−15 460/T) min^{-1}
k_{p0} =	3×10^9 exp (−3320/T) L/(mol·min)
k_p =	k_{p0} exp [0.2(1/V_f − 1/V_{fcr})]
k_{tm} =	5.78 exp (−2768/T)k_p
k_{tp} =	$0.32k_{tm}$ (at 50°C)
k_{t1} =	7.8×10^{13} exp (−2190/T) L/(mol·min)
k_{t20} =	k_{t1}/P^2
V_0 =	5 L
V_{fcr} =	V_f at x_f
Z =	0.98

The free volume fraction of the reacting mixture in the polymer-rich phase, V_f, can be calculated by

$$V_f = \alpha x + \beta. \tag{80}$$

$V_{f,cr}$ denotes the critical value of V_f beyond which the propagation rate constant becomes diffusion controlled. Expressions (79) and (80) also contain Parameter A, the value of which has to be estimated together with the values of α, β, and $V_{f,cr}$ from experimental data on conversion and molecular weight averages.

Conversion profiles and polymerization rates generated by the solution of Models A, B, and C are compared to those obtained by the present model in Figs. 1 and 2. Note that the results obtained by the present model are identical to those of Model D provided that exactly the same kinetic parameters are used. This must be so since both models result in identical expressions for the rate of monomer conversion. From Figs. 1 and 2 it can be seen that in the conversion range $0 < x \leq x_c$, all models show almost identical behavior since the derived rate Expressions (38), (64), (74), and (77)

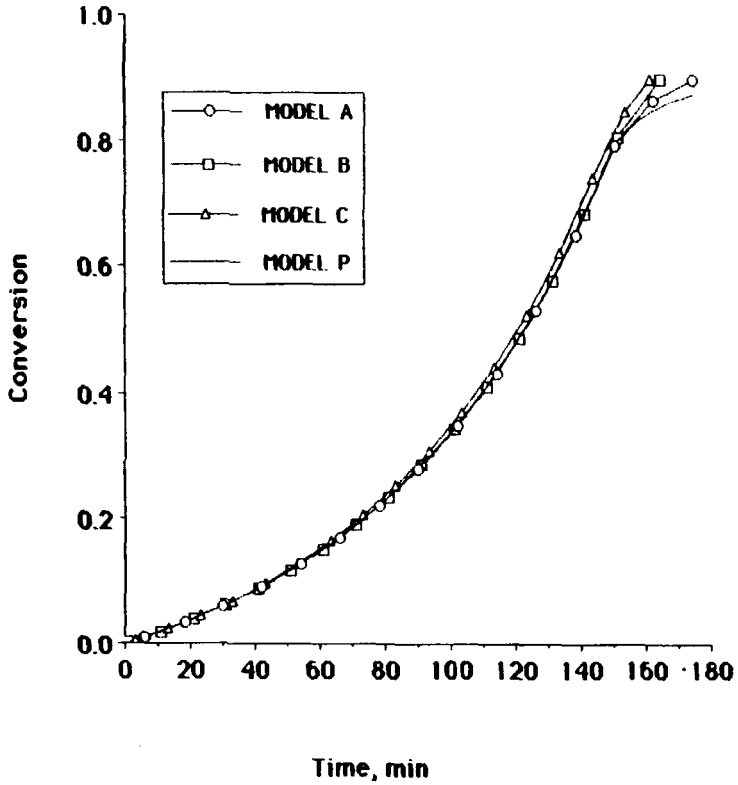

FIG. 1. Comparison of various conversion profiles obtained by solution of Models A, B, and C and the present model (P). $T = 50°C$, $I_0 = 0.2$ mol.

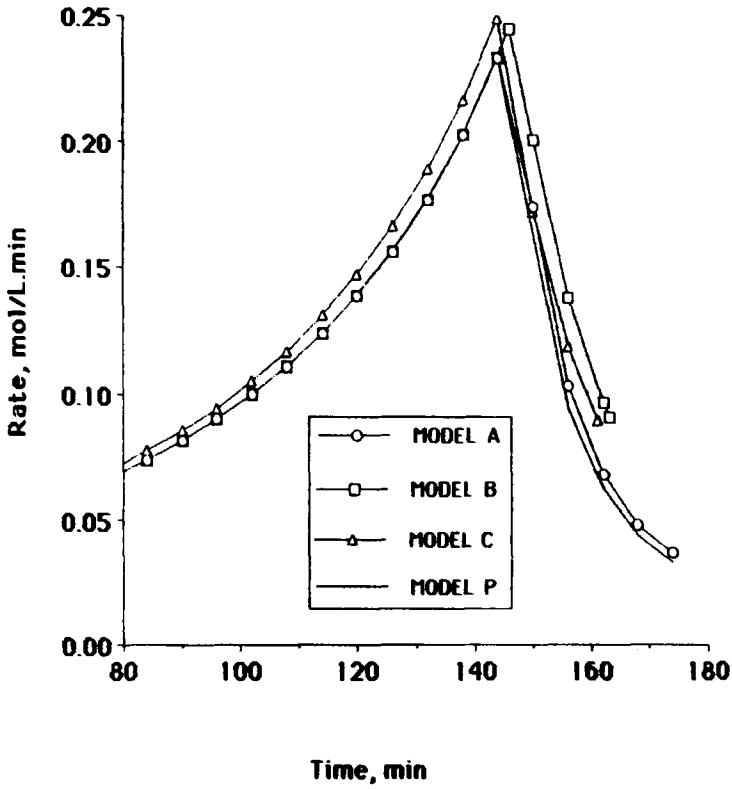

FIG. 2. Comparison of rate of polymerization profiles obtained by the solution of Models A, B, and C and the present model (P) (cf. Fig. 1). T = 50°C, I_0 = 0.2 mol.

are very similar. The differences observed between the predictions of the various models for conversions greater than x_c are primarily due to diffusion control of the termination and propagation reactions. In fact, Models B and C assume that k_t and k_p remain constant during the course of the polymerization. Model A includes an empirical correction factor to account for the changes in k_t and k_p at high conversions. The present model assumes that k_t and k_p change according to Eqs. (78) and (79).

It should be pointed out that Models A–C make use of the QSSA in deriving the equation for the polymerization rate. On the other hand, Model D and the present model do not necessarily require the use of the QSSA because differential equations for the moments of the growing polymer distributions are also included in the model. The validity of the QSSA was tested by solving the present model equations with or without the use of the QSSA. In the former case the differential equations for the moments of the live macroradicals were replaced by corresponding algebraic equations. No significant differences were observed between the two solutions, which justifies the use of the QSSA for conversion predictions under the tested experimental conditions.

Prediction of Molecular Properties

Prediction and control of molecular weight averages, number of short- and long-chain branches, and terminal double bonds per polymer molecule is of considerable importance to the PVC industry since the low thermal stability of PVC has been linked to the formation of some branched and unsaturated molecular structures mainly generated by chain transfer to monomer. In vinyl chloride polymerization, the molecular weight distribution (MWD) and molecular weight averages are actually controlled by transfer to monomer and are almost independent of initiator concentration and monomer conversion up to a conversion of about 0.85. In this conversion range the MWD of polymer will be given by the most probable distribution, and the polydispersity index ($\bar{M}_w/\bar{M}_n$) will be very close to 2. However, as the monomer conversion increases, the relative rates of the various free-radical reactions that control the molecular structure of PVC chains change due to the appearance of strong diffusion control. In this conversion region the amount of long- and short-chain branches increases as well as the production of low molecular weight polymer chains. This might result in an increase of the polydispersity index from 2 to a value as high as 3 and cause a deterioration of the thermal stability of the PVC. In what follows, simulation results are presented showing the effects of a diffusion-controlled propagation and transfer to polymer on the molecular properties of PVC. In all simulations it is assumed that the termination reaction is controlled by the diffusion of large live macroradicals (see Eq. 78).

Under diffusion-controlled conditions of the propagation rate constant (Fig. 3, Curve b), $\bar{M}_n$ decreases as the conversion increases due to the production of low molecular weight polymer. This is better seen in Fig. 4 which shows the *instantaneous* number-average molecular weight which, under diffusion-controlled conditions, is seen to significantly decrease with conversion. It should be pointed out that these results are only indicative of the actual trends one can expect for $\bar{M}_n$ at very high conversions. As expected, $\bar{M}_n$ will not be affected by transfer to polymer.

Curves a and b in Figs. 5 and 6 show the effect of transfer to polymer on $\bar{M}_w$ and $\bar{M}_{w,i}$ with or without the application of a diffusion correction factor to the propagation

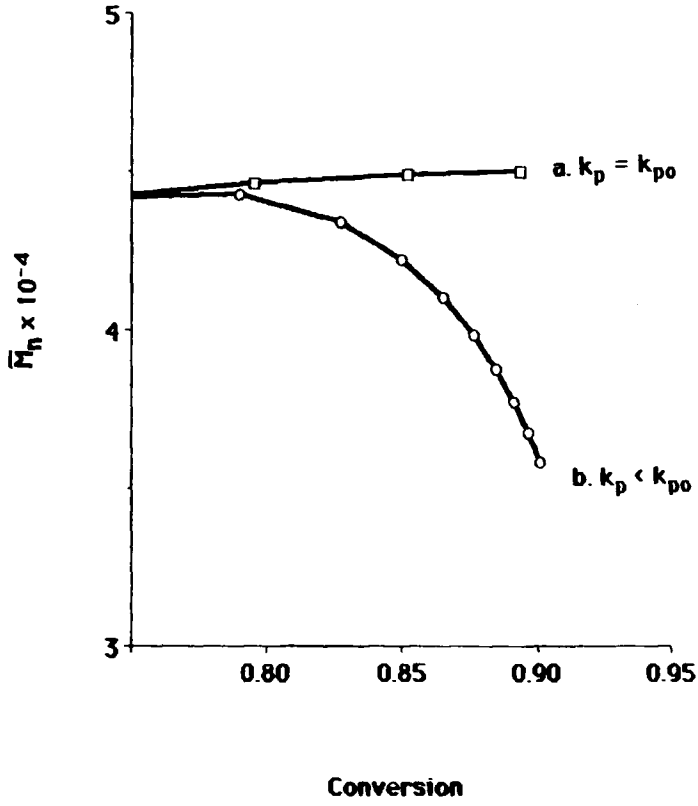

FIG. 3. Effect of diffusion-controlled propagation rate constant on the cumulative number-average molecular weight, $\bar{M}_n$ (simulation conditions as in Fig. 1).

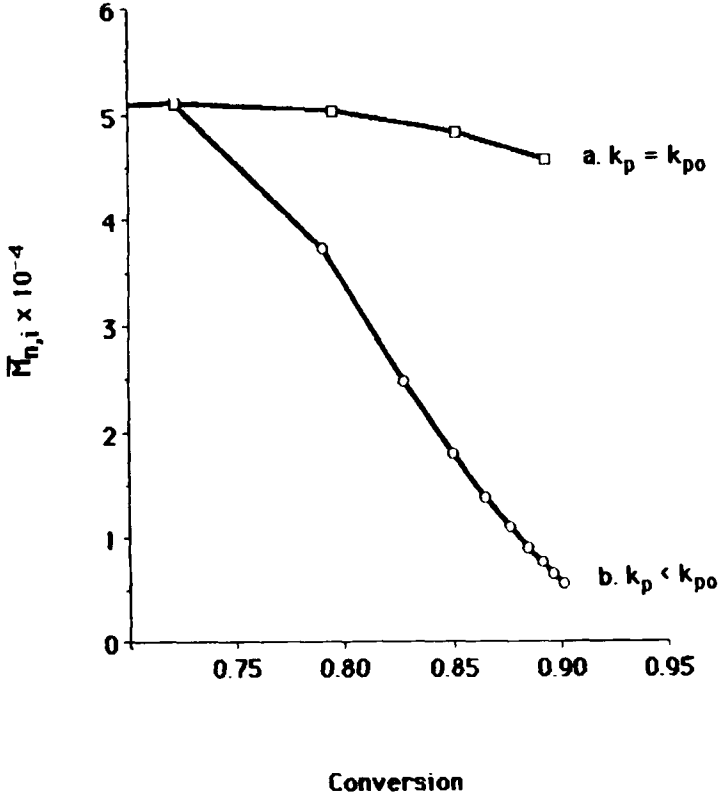

FIG. 4. Effect of diffusion-controlled propagation rate constant on the instantaneous number-average molecular weight, $\bar{M}_{n,i}$ (cf. Fig. 3).

rate constant. It is clear that transfer to polymer results in a significant increase in $\bar{M}_w$ and $\bar{M}_{w,i}$ in both cases, but no significant change with conversion is observed in the absence of transfer to polymer reaction ($k_{tp} = 0$) and diffusion invariable propagation reaction ($k_p = k_{p0}$), Case c in Figs. 5 and 6. As in Figs. 3 and 4, a decrease in the propagation rate constant results in a decrease in $\bar{M}_w$ and $\bar{M}_{w,i}$ (Case d). The corresponding variation of the polydispersity index with conversion, plotted in Fig. 7, demonstrates that the incorporation of both transfer to polymer and diffusion-controlled propagation results in a significant increase in the polydispersity index at high conversions (Case b), yet it remains practically constant under the assumptions of constant $k_p = k_{p0}$ and zero $k_{tp} = 0$ (Case c).

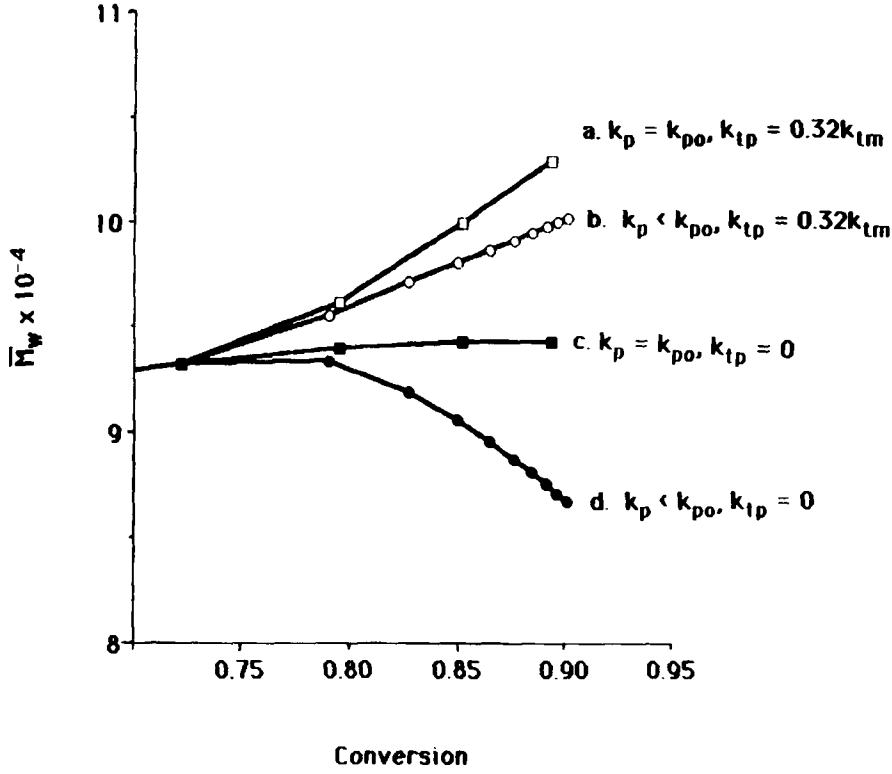

FIG. 5. Effect of transfer to polymer and propagation on the cumulative weight-average molecular weight, $\bar{M}_w$ (simulation conditions as in Fig. 1).

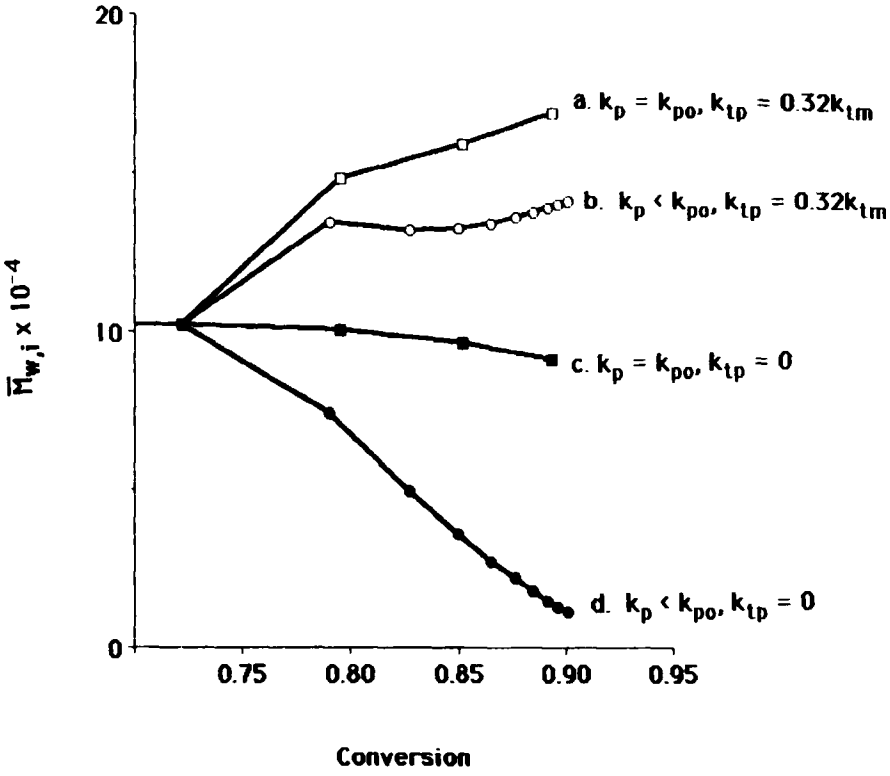

FIG. 6. Effect of transfer to polymer and propagation on the instantaneous weight-average molecular weight, $\bar{M}_{w,i}$ (cf. Fig. 3).

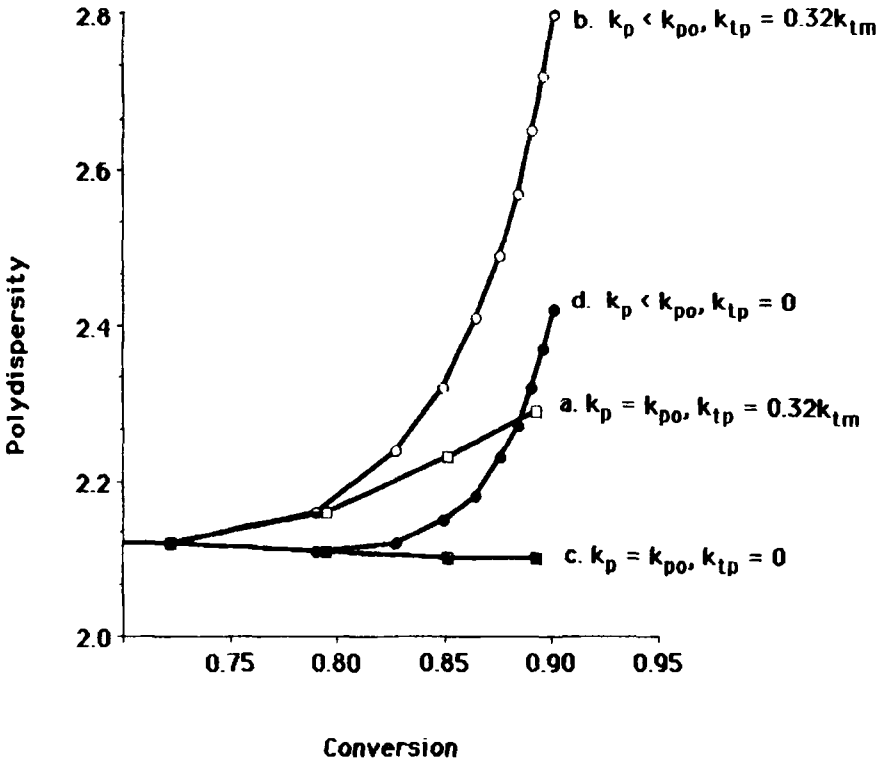

FIG. 7. Effect of transfer to polymer and propagation on the polydispersity index ($\bar{M}_w/\bar{M}_n$) (cf. Figs. 3 and 5).

Figure 8 shows that for constant k_p (Curve a), the number of SCB increases only slightly with conversion to ~2 branches per 1000 carbon atoms. On the other hand, a variable k_p (Curve b) results in a significant increase in the number of SCB, especially at high conversions. This agrees with various experimental observations which show an average of 4–5 chloromethyl branches per 1000 monomer units. The number of LCB does not vary up to a conversion at which the separate monomer phase disappears. However, under monomer-starved conditions, the LCB increases, which has been confirmed experimentally. A diffusion-controlled propagation reaction results in a higher degree of branching (Curve d).

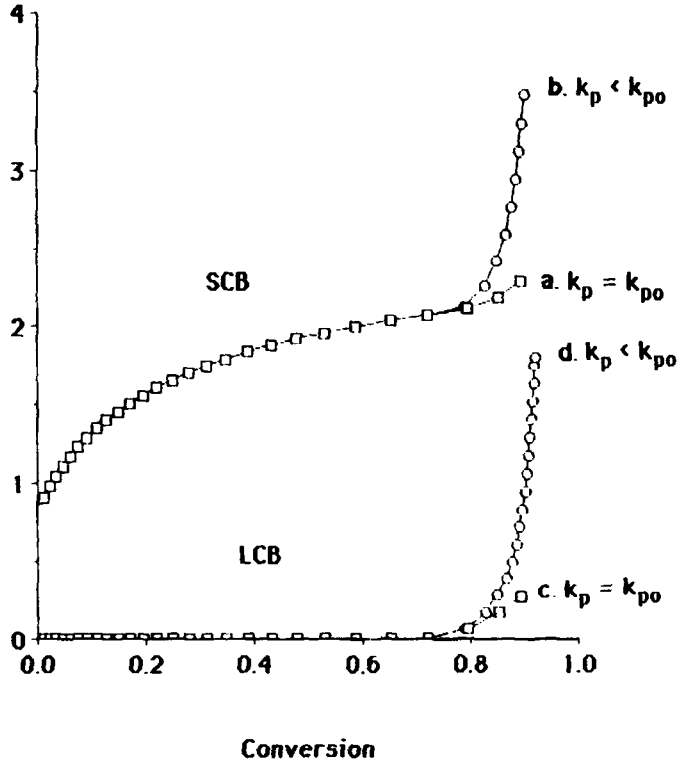

FIG. 8. Effect of propagation rate constant on the number of short-chain branches (SCB) and the number of long-chain branches (LCB) per 1000 carbon atoms as a function of monomer conversion (simulation conditions as in Fig. 1).

Figure 9 shows a limiting value of about 0.95 terminal bonds per molecule is reached and remains almost unchanged after conversion x_c. Hjertberg and Sörvik [1] found a linear relation between $\bar{M}_n$ and the number of double bonds for both saturated and unsaturated PVC samples. For a polymer with a $\bar{M}_n$ 50 000, they found approximately one terminal double bond per molecule, in close agreement with the results of Fig. 9. Notice that the net rate of formation of terminal double bonds was calculated by

$$d(db)/dt = r_t + Zr_{tm}, \tag{81}$$

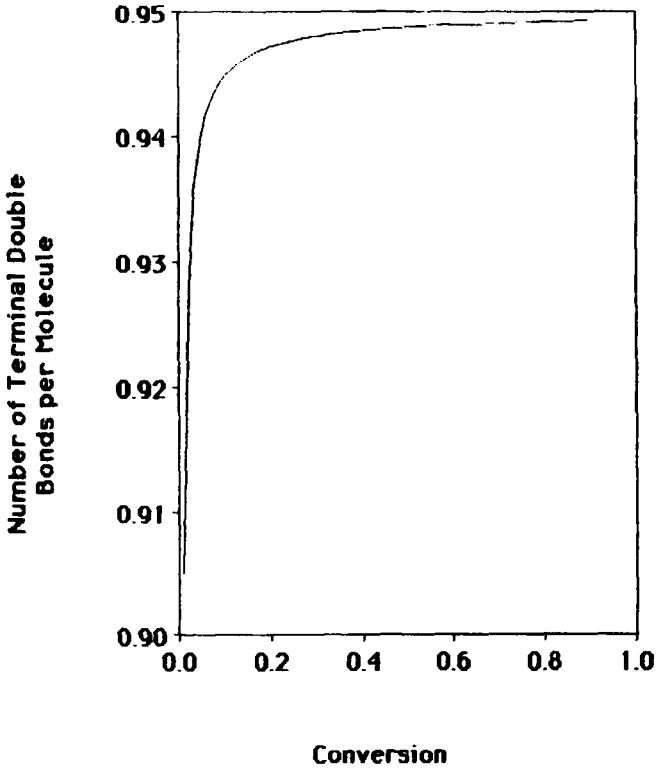

FIG. 9. Variation of the number of terminal double bonds per molecule with monomer conversion (simulation conditions as in Fig. 1).

where r_t is the total termination rate by disproportionation and r_{tm} is the total rate of transfer to monomer, while Z is a constant representing the fraction of all transfer to monomer reactions leading to the formation of terminal double bonds. Equation (81) is in agreement with the experimental results of Hildenbrand et al. [7], who found that the number of terminal double bonds per molecule in PVC was proportional to the number of polymer molecules and always less than unity (0.85–0.95).

In Figs. 10 and 11 the number- and weight-average molecular weights calculated by Eqs. (69) and (70) are compared to molecular weight results obtained by the present model without the use of the QSSA. It should be mentioned that Expressions (69) and (70) have been derived under QSSA throughout the course of the polymerization. As can be seen, no significant differences exist between the two approaches

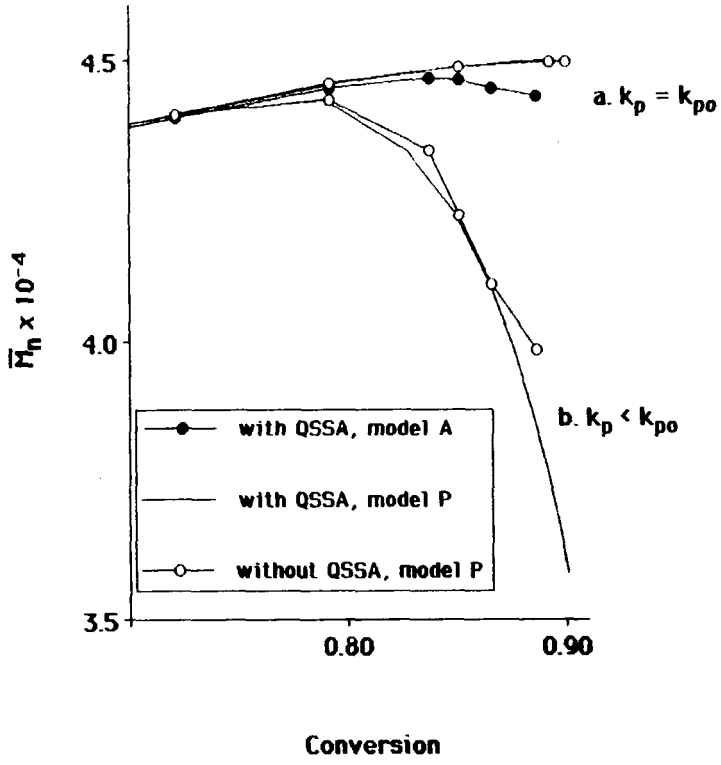

FIG. 10. Comparison of $\bar{M}_n$ profiles obtained by the instantaneous method (Model A) and the present model with/without the application of QSSA (simulation conditions as in Fig. 1).

up to a conversion of 0.9, which supports the validity of QSSA for the experimental conditions tested.

It should be clear that all simulation results presented in this paper are only indicative of the real trends expected in a PVC process. However, the present analysis has demonstrated the ability of the new model to predict the polymer quality of the resin produced as a function of the process conditions. Furthermore, the present model, in close relation to experimental observations, can significantly contribute to the elucidation of the various possible mechanisms that have been proposed to explain the two-phase polymerization of VC and the formation of anomalous structures in PVC.

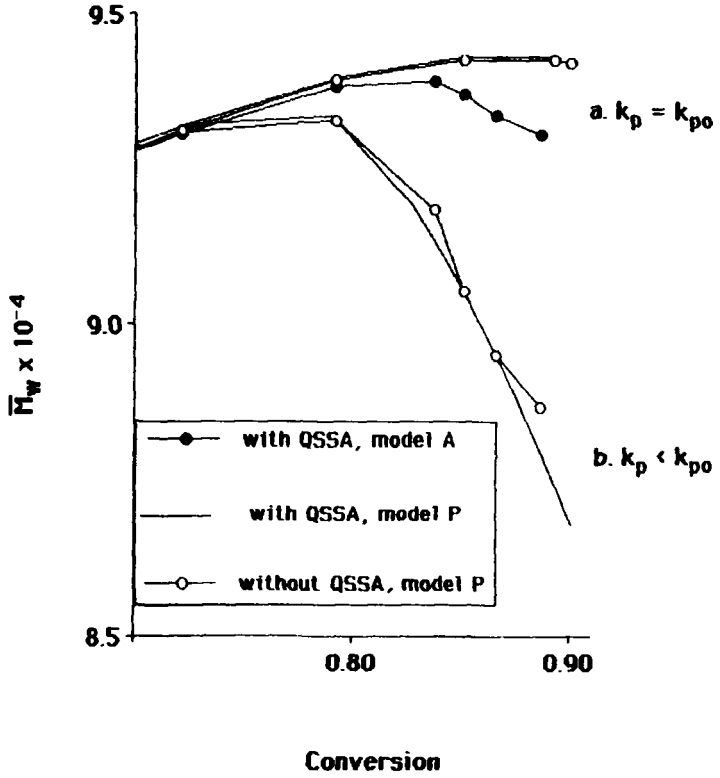

FIG. 11. Comparison of $\bar{M}_w$ profiles obtained by the instantaneous method (Model A) and the present model with/without the application of QSSA (simulation conditions as in Fig. 1).

NOMENCLATURE

I	moles of initiator
f	initiator efficiency
k_b	rate constant for short-chain branching (s^{-1})
k_d	rate constant for decomposition of initiator (s^{-1})
k_i	rate constant for chain initiation (s^{-1})
k_{ma}	radical absorption mass transfer coefficient (L/s)
k_{md}	radical desorption mass transfer coefficient (L/s)

k_p	rate constant for chain propagation (L/(mol·s))
k_{tc}	rate constant for termination by combination (L/(mol·s))
k_{td}	rate constant for termination by disproportionation (L/(mol·s))
k_{tm}	rate constant for chain transfer to monomer (L/(mol·s))
k_{tp}	rate constant for chain transfer to polymer (L/(mol·s))
k_t	$k_{tc} + k_{td}$
K_s	partition coefficient of Species s between Phases 1 and 2
$\bar{L}_N$	average number of long branches per polymer molecule
M	moles of monomer
$\bar{M}_n$	number-average molecular weight
$\bar{M}_w$	weight-average molecular weight
(MW)	molecular weight of monomer
R_x	number of growing radicals of chain length x
$\bar{S}_N$	average number of short branches per polymer molecule
V	volume of reacting mixture
V_f	free volume fraction of reacting mixture
x	fractional monomer conversion
$\bar{x}_n$	instantaneous number-average chain length
$\bar{x}_w$	instantaneous weight-average chain length
$\bar{X}_n$	cumulative number-average chain length
$\bar{X}_w$	cumulative weight-average chain length
T	reactor temperature

Greek

λ_{ij}	ith moment of live polymer distribution
μ_{ij}	ith moment of dead polymer distribution
ρ_m	density of monomer (g/L)
ρ_p	density of polymer (g/L)
ϕ_s	volume fraction of Species s

REFERENCES

[1] T. Hjertberg and E. M. Sörvik, *J. Macromol. Sci.—Chem., A17*(6), 983 (1982).
[2] A. E. Hamielec, R. Gomez-Vaillard, and F. L. Marten, *Ibid., A17*(6), 1005 (1982).
[3] A. A. Caraculacu, *Pure Appl. Chem., 53*, 398 (1981).

[4] W. H. Starnes, F. C. Schilling, I. M. Plitz, R. E. Cais, D. J. Freed, R. L. Hartless, and F. A. Bovey, *Macromolecules, 16,* 790 (1983).
[5] T. Hjertberg and E. M. Sörvic, *J. Polym. Sci., Polym. Chem. Ed., 24,* 1313 (1986).
[6] T. Hjertberg and E. M. Sörvic, *J. Vinyl Technol., 7*(2), 53 (1985).
[7] P. Hildenbrand, W. Ahrens, F. Brandstetter, and P. Simak, *J. Macromol. Sci.—Chem., A17*(6), 1093 (1982).
[8] J. Ugelstad, *Ibid., A11,* 1281 (1977).
[9] J. Ugelstad, P. C. Mork, and F. K. Hansen, *Pure Appl. Chem., 53,* 323 (1981).
[10] A. Crosato-Arnaldi, P. Gasparini, and G. Talamini, *Makromol. Chem., 117,* 140 (1968).
[11] A. H. Abdel-Alim and A. E. Hamielec, *J. Appl. Polym. Sci., 16,* 783 (1972).
[12] J. Ugelstad, H. Flogstad, T. Hertzberg, and E. Sund, *Makromol. Chem., 164,* 171 (1973).
[13] S. J. Kuchanov and D. N. Bort, *Polym. Sci. USSR, 15,* 2712 (1973).
[14] O. F. Olaj, *Angew. Makromol. Chem., 1,* 47 (1975).
[15] R. Thiele, J. Nelles, and D. Rauchstein, *Plaste Kautsch., 7,* 395 (1978).
[16] V. V. Kafarov, I. N. Dorokhov, A. A. Dudorov, and P. Kusy, *Dokl. Akad. Nauk SSSR, 243,* 711 (1978).
[17] D. G. Kelsall and G. C. Maitland, in *Polymer Reaction Engineering. Influence of Reactor Engineering on Polymer Properties* (K. H. Reichert and W. Geiseler, eds.), Hansen, 1983.
[18] M. Tirell, R. Galvan, and R. L. Laurence, in *Chemical Reaction and Reactor Engineering* (J. J. Carberry and A. Varma, eds.), Dekker, New York, 1987.
[19] B. Törnell, *Polym.-Plast. Technol. Eng., 27*(1), 1 (1988).
[20] J. A. Biesenberger and D. H. Sebastian, in *Principles of Polymerization Engineering,* Wiley, New York, 1983.
[21] F. L. Marten and A. E. Hamielec, *J. Appl. Polym. Sci., 27,* 489 (1982).

Received November 28, 1988
Revision received March 31, 1989